Preprints, 4th IFAC Conference on
Advances in Proportional-Integral-Derivative Control
Almería, Spain | June 12-14, 2024

Coupled Continuous PID Controllers for the IFAC Benchmark on Vapor Compression Refrigeration on the Behavioural Setting

Jesús-Antonio Hernández-Riveros*, Gerardo J. Amador Soto**

Universidad Nacional de Colombia, Medellín. Facultad de Minas, Departamento de Energía Eléctrica y Automática. Colombia.
* (jahernan@unal.edu.co)
** (gjamadors@unal.edu.co)

Abstract: This paper presents a behavioral-based controllers design, utilizing evolutionary learning of trajectories, applied to the IFAC PID18 benchmark model for a vapor compression refrigeration system. The challenge of tracing both the evaporator outlet temperature (Te,sec,out) and superheat temperature (Tsh) with disturbances and imposed restrictions is addressed. The challenge integrates a preset discrete MIMO control scheme, serving as a basis for comparison with alternative control schemes. The proposed method also allows for direct experimentation on the system, bypassing the need for reference models or mathematical representations. By developing behavioral paths and iteratively adjusting controller variables, satisfactory control objectives are achieved. The evolutionary behavioral approach is tested on the default discrete control scheme and then applied to newly designed coupled continuous PID controllers, which outperform the benchmark strategy. The method is versatile, adaptable to both model-based and data-driven approaches, and offers a direct relationship with the physical system, independent of both its representation and controller structure, thus emulating real-world conditions effectively.

Keywords: Behavioral control, learning and adaptive systems, evolutionary algorithms, refrigeration.

1. Introduction

The main purpose of a vapor compression refrigeration system (VCRS) is to extract and transfer heat from a cold compartment to its surroundings at a higher temperature using mechanical components (see **Fig. 1**).

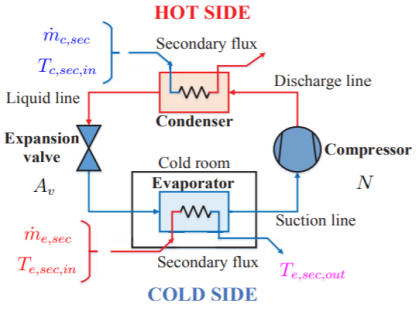

Fig. 1. VCRS depiction. Taken from (Bejarano et al., 2018).

Traditionally, enhancing energy efficiency in VCRSsystems involves redesigns, new materials, new technologies, and best practices. In the industry, a practical approach is to operate the cycle with a specific superheating temperature (Tsh) for the refrigerant at the evaporator outlet. This indirectly boosts energy efficiency by raising the coefficient of performance (COP). Recent advancements like variable speed compressors and electronic expansion valves allow gradual intervention in the process, opening avenues for direct energy consumption reduction. Research is seeking intelligent control structures to manipulate these elements effectively. The challenge is to couple these technologies to improve temperature control precision and lower total energy usage. In the PID 18 challenge, a VCRS model facilitates assessing controller designs' accuracy by tracking both operating evaporator temperature and superheat temperature, thus indirectly reducing energy consumption (Bejarano et al., 2018).

This paper outlines the performance of a behavior-based control method, employing evolutionary learning of trajectories, applied to the IFAC18 benchmark model of a VCRS. The benchmark already includes a preset MIMO discrete control scheme. Similar proposals addressing the design and tuning of a coupled multivariable controller have been presented in (Hernández-Riveros et al., 2016; Zeng et al., 2015). The evolutionary technique enables the discovery of practical solutions without significantly complicating the initial problem, regardless of the plant model and control scheme structure. Consequently, the original discrete control scheme will be substituted with two coupled continuous PID controllers. The method's applicability to the original problem and its independence and attributes are demonstrated.

The structure of this paper is as follows: benchmark model and its control scheme are described in detail in section 2. The behavior-based control evolutionary technique proposal applied to the benchmark is introduced in section 3. In section 4, a comparative evaluation and analysis of the multivariable controllers found is done. Section 5 summaries the concluding remarks of this work

2. About the PID18 benchmark model and control scheme

Modeling the dynamics of a VCRS presents significant challenges due to the complex interaction of various forms of energy. Key considerations include high thermal inertia, strong component coupling, nonlinearities, uncertainties, disturbances, and dead times. The benchmark plant model, based on the switched moving-boundary approach, encompasses one compression stage and a refrigeration load-

demand system (Li et al., 2012). Simulations span 20 minutes of continuous operation, with the heat exchanger divided into zones representing different refrigerant states. The model, designed for control purposes, explicitly outlines manipulated variables and major disturbances. It serves as a tool to evaluate system energy efficiency relative to desired outputs given available inputs.

2.1 MIMO refrigeration control system

As mentioned before, the benchmark model is control oriented integrating a preset discrete MIMO control scheme. Choosing the structure of the multivariable control is totally free in the challenge. The controllers could be discrete, continuous, or hybrid. This benchmark model and MIMO control scheme provides a suitable scenario to evaluate the effectiveness of a technique regardless of the selected control structures and the complexity of the model.

2.2 Control scheme description

The control scheme on the benchmark is conventional. Control objectives are stablished imposing a reference by the cooling demand (Te,sec,out), and also a set point (low but constant) on the degree of superheating (Tsh) (see **Fig. 2)**. The controllers are designed to track the references of these two variables manipulating, in presence of disturbances, the aperture of the expansion valve and the compressor speed (see **Table 1** and **Table** 2). Constraints ranges on the manipulated variables are also considered.

Table 1. Input and output variables.

Input variables	**Symbol**	**Unit**
Expansion valve aperture	Av	%
Compressor speed	N	Hz
Output variables	**Symbol**	**Unit**
Outlet temperature of the evaporator secondary fluid	Te,sec,out	ºC
Super heat temperature	Tsh	ºC

Table 2
Disturbance variables

Disturbances	**Symbol**	**Unit**
Inlet temperature of the condenser secondary flux	Tc,sec,in	ºC
Mass flow of the condenser secondary flux	$\dot{m}$c,sec	g s-1
Inlet pressure of the condenser secondary flux	Pc,sec,in	bar
Inlet temperature of the evaporator secondary flux	Te,sec,in	ºC
Mass flow of the evaporator secondary flux	$\dot{m}$e,sec	g s-1
Inlet pressure of the evaporator secondary flux	Pe,sec,in	bar
Compressor surroundings temperature	Tsurr	ºC

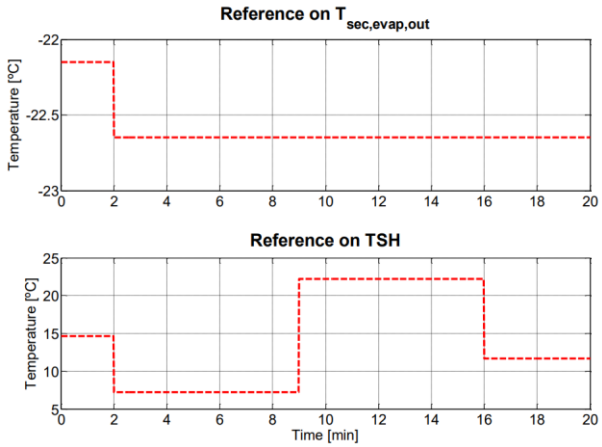

Fig. 2. Changes in the references for each output variable. Taken from (Bejarano et al., 2018).

2.2 Other control techniques approaches

According to (Zardini, 2017), in general, the control strategies can be divided into two viewpoints:

1. Avoid the MIMO complexity by applying SISO controllers, e.g.: a) Decentralized control, b) Pairing problem, c) Decoupled control.
2. Centralized multivariable control, optimizing some cost function, e.g.: a) Linear Quadratic Regulator, b) H-infinity control.

Linear modelling of VCRS can face challenges, such as closed-loop instability due to high coupling between variables, dead times, thermal inertia, and nonlinearities (Bejarano et al., 2018). Controllers must be robust to handle these conditions, even at operating points far from the desired behavior. Proposed methods need to address this complex scenario effectively.

3. Coupled controllers design through behavior-based approach

The behavior-based approach for dynamical systems is notable for its direct connection to the plant, allowing representation-free solutions. It enables the generation of information for general or specific conditions. According to this approach, the behavior ($\mathcal{B}$) of a dynamical system is a set of trajectories (Willems, 2007). A dynamical system is defined as $\sum = (\boldsymbol{T}, \boldsymbol{W}, \mathcal{B})$, where, $\boldsymbol{T}$ is the time axis, $\boldsymbol{W} \in \mathbb{R}^{q}$ is the signal space, and $\mathcal{B} \subset \mathbb{R}^{q^{\mathbb{Z}}}$ is the associated space of trajectories. Each $w(i)$ can be partitioned in a permutation matrix $P = \begin{bmatrix} u(i) \\ y(i) \end{bmatrix}$ where $u(i) \in \mathbb{R}^{m}$ and $y(i) \in \mathbb{R}^{q-m}$ are free (inputs) and dependent (outputs) variables.

The behavior of a real plant, $\mathcal{B}_{\text{plant}}$, encompasses constraints, bounds, variable saturation, and specific capabilities. In the behavioral approach, only trajectories meeting the plant's conditions are considered, ensuring feasible and safe solutions. Hence, a real plant trajectory has a fixed length, L, so that, $\mathcal{B}_{plant} \subset \mathbb{R}^{qL}$. A real plant is a dynamical system given by $\boldsymbol{\Sigma}_{plant} = (\boldsymbol{T}, \boldsymbol{W}, \mathcal{B}_{plant})$.

From the behavioral point of view, a controller, is another dynamical system, $\boldsymbol{\Sigma}_{controller} = (\boldsymbol{T}, \boldsymbol{K}, \mathcal{B}_{controller})$, in

interconnection with the plant. $\boldsymbol{K}$ is the signal space of control variables in the same time axis $\boldsymbol{T}$. As a plant, a controller has its own conditions of behavior, $\mathcal{B}_{controller}$, but imposes restrictions on the plant only through admissible plant trajectories, $\boldsymbol{W} \in \mathbb{R}^{qL}$.

A full behavior is defined by $\mathcal{B}_{\text{full}} = \{(w,k): \boldsymbol{T} \to \boldsymbol{W}\boldsymbol{X}\boldsymbol{K} | (w,k) \in \mathcal{B}_{plant}$ and $k \in \mathcal{B}_{controller}\}$, a controlled system is $\Sigma_{controlled} = (\boldsymbol{T}, \boldsymbol{W}, \mathcal{B}_{controlled})$ with $\mathcal{B}_{controlled} = \{w: \boldsymbol{T} \to \boldsymbol{W} | k: \boldsymbol{T} \to \boldsymbol{K}$ such that $(w,k) \in \mathcal{B}_{plant}$ and $k \in \mathcal{B}_{controller}\}$. Knowing the own operating conditions of the full system, the behavioral approach in control systems may be applied based on model or based on data.

Evolutionary learning of trajectories facilitates the identification of potential behavioral paths that align with control objectives, irrespective of model complexity, domain, structure, or purpose. Traditionally, control engineering tackles this by employing a reference model of a VCRS to tune controllers using model information. However, in this paper, the IFAC18 benchmark model serves solely as a data generator for independent and dependent variables. The evolutionary approach mimics direct manipulation within the process, gathering knowledge/experience to enhance temperature control precision, as illustrated in **Fig. 3**.

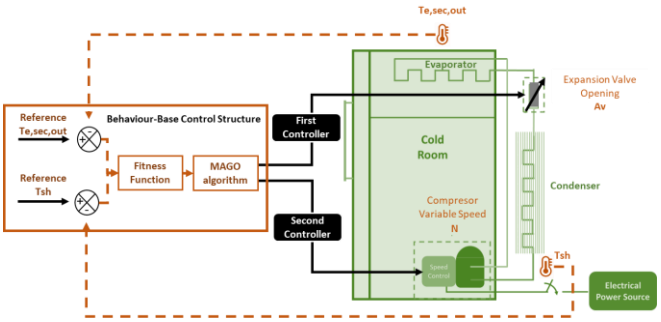

Fig. 3. Direct intervention on the VCRS using the behavior-based approach, regardless of the controller type

The behavior-based control structure employs sensors to gather system variables and assesses error margins using logical operators. This information is used to construct a cost function, guiding input actions based on control objectives and generating a performance index like ITAE. The intelligent control structure then utilizes three population dynamics within an evolutionary search process to propose optimal controller parameter combinations, aiming to minimize error. Facilitating this task is the auto-organized evolutionary algorithm MAGO, which effectively navigates the complex environment characterized by strong internal variable relationships and the intricate MIMO control problem. MAGO utilizes statistical operators instead of genetic ones. Use of statistical operators, along with the covariance matrix of the population, enables efficient management of variable interrelationships and dependencies.

3.1 Multidynamics algorithm for global optimization – MAGO.

MAGO, an auto-organized real-value evolutionary algorithm, operates with just two external parameters: population size (Pob) and number of generations (Ng). Each generation comprises two stages: one for competition and the other for adaptation. MAGO strategically evolves the population based on statistical insights drawn from its covariance matrix. Its efficacy in solving engineering problems has been demonstrated (Balarezo-Gallardo & Hernández-Riveros, 2017; Soto et al., 2018). Unlike typical evolutionary algorithms, MAGO employs three distinct autonomous dynamics to balance exploration and exploitation, mitigating the risk of converging to local optima. It calculates statistics of the population to autonomously divides it into three subgroups: Emergent Dynamics, Crowd Dynamics, and Accidental Dynamics. Each subgroup undergoes its own evolutionary process. After evaluating fitness functions, the population is rearranged from best to worst individuals. This rearrangement is akin to a normal distribution, determining subgroup cardinalities based on each standard deviation. The cardinalities' magnitude changes in each generation. The resulting groups are expressed in equations **Eqs. (1)-(3)**, where the mean of the actual population is $x_M^{(j)}$, the sample covariance matrix of the population in generation j is $S^{(j)}$ and the entire population is $Pob^{(j)} = G1 \cup G2 \cup G3$.

$$G_1 = \left\{ \boldsymbol{x} \in \frac{Pob^{(j)}}{x_M^{(j)}} - \sqrt{diag(S^{(j)})} \leq \boldsymbol{x} \geq x_M^{(j)} + \sqrt{diag(S^{(j)})} \right\} \quad (1)$$

$$G_2 = \left\{ \boldsymbol{x} \in \frac{Pob^{(j)}}{x_M^{(j)}} - 2\sqrt{diag(S^{(j)})} \leq \boldsymbol{x} \geq x_M^{(j)} + \sqrt{\text{diag}(S^{(j)})} \right\} \quad (2)$$

$$G_3 = \left\{ \begin{matrix} \boldsymbol{x} \in \frac{Pob^{(j)}}{x} \leq x_M^{(j)} - 2\sqrt{diag(S^{(j)})}; \\ \boldsymbol{x} \geq x_M^{(j)} + 2\sqrt{diag(S^{(j)})} \end{matrix} \right\} \quad (3)$$

In each generation, MAGO produces new individuals. through those dynamics. A subset for the new population is produced by each dynamic. Emergent Dynamic manages an elite neighborhood seeking solutions closer to the very best individual, applying the Nelder-Mead method of numerical derivation, **Eq. (4)**. Making a faster convergence of the algorithm and keeping an equilibrium between exploitation and exploration over the searching space, is part of the role of this dynamic.

$$x_T^{(j)} = x_i^{(j)} + F^{(j)} \times (x_B^{(j)} - x_m^{(j)}) \quad (4)$$

The distance between the best individual of generation j, $x_B^{(j)}$, and a randomly chosen individual from the Emergent Dynamic, $x_i^{(j)} = x_m^{(j)}$, is weighted by a factor $F^{(j)}$ that includes information about the problem variables from the covariance matrix of the actual population, **Eq. (5)**.

$$F^{(j)} = \frac{S^{(j)}}{\|S^{(j)}\|} \quad (5)$$

The upper and lower limits from the second dispersion, [$LB^{(j)}$, $UB^{(j)}$], and the mean of the current population are used to sample a uniform distribution to determine the individuals produced by the Crowd Dynamic. This dynamic holds the memory of the evolution process. In contrast, sampling from a uniform distribution throughout the whole searching space produces the individuals of the Accidental Dynamic. The cardinality of this dynamic is smaller. This dynamic helps to maintain the diversity of the population and ensures numerical stability of the algorithm. MAGO pseudocode is below.

MAGO algorithm

1: j:= 0; Initiate population from a uniform distribution over the search space.
2: Repeat
3: Fitness function evaluation of each individual.
4: Calculation of the mean, covariance matrix, first, second and third dispersion of the actual population.
5. Reorganization of the population from the best to the worst fitness function.
6: Cardinalities calculation of the 3 dynamics (N1, N2, N3).
7: Selection of N1 best individuals, moving toward the best of all upon equation 4. After competing with their parents, the best of both is chosen to next generation.
8: Sample N2 individuals with a uniform distribution in the hyper volume [$LB^{(j)}$, $UB^{(j)}$], pass them to next generation.
9: With a uniform distribution over the entire search space, sampling N3 individuals and pass them to next generation.
10: j = j + 1
11: Until satisfy a stopping criterion.

As in other evolutionary algorithms, due to its stochastic nature, calculating the computational complexity of MAGO is not an easy task. Also, the fitness function depends on each problem. The MAGO works with real numbers, so the size of each variable depends on the operating system, and the evolutionary operators are statistical, so both can be considered to have fixed behavior, in this way the computational complexity, big-O, of the MAGO depends only on the number of generations, *Ng*, and the population size, *Pob*, that is, the computational complexity of MAGO can be close to O(*NgPob*). Since Emerging Dynamics is an elite-type treatment of the best individuals, convergence to a feasible solution is guaranteed. A performance evaluation of MAGO is found in (Hernández-Riveros, 2012).

3.2 Evolutionary coupled control tuning scenarios

For control problems a reference behaviour is needed describing a L-length reference trajectory w_r. The control is the finite-time optimization problem: minimize K_{ctrl} (w, w_r) subject to $w_r \in \mathcal{B}_{\text{plant}}$. The most important part of w_r is the sequence of the dependent variable, y_r, and the control problem is rewrite as minimize $\boldsymbol{K}_{ctrl}$ (y, y_r). The minimizer is denoted as y^*. Open-loop control is finding a u_i such that (y_i, y_r) $\leq \varepsilon$. Closed-loop control is finding the parameters of a controller structure such that exist a y^*, and (y^*, y_r) $\leq \varepsilon$, with a u_i=f (controller structure) and $y^* = y_i$.

Two scenarios are proposed to verify both the effectiveness in the design of controllers and the independence of the evolutionary learning of behaviours technique around the structure used for its implementation on the IFAC18 benchmark model of a VCRS. The first scenario uses the default discrete transfer function controllers from the benchmark. The second scenario finds two new continuous coupled PID controllers (see **Fig. 4**). Given MAGO is a real-valued evolutionary algorithm, a vector containing the parameters of the two controllers is enough to represent the evolutionary individual.

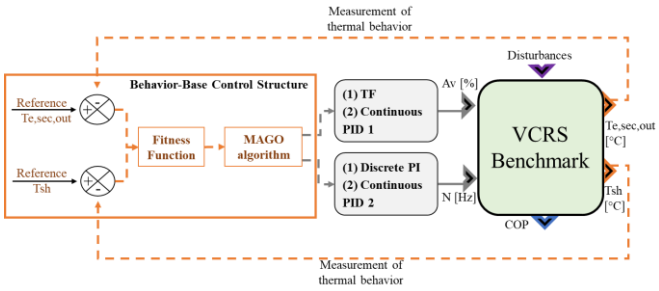

Fig. 4. Coupled evolutionary tuning for the benchmark using the behavior-based approach: (1) preset discrete MIMO control scheme and (2) continuous PID controllers.

For the first scenario, the structure of the evolutionary individual corresponds to the terms of the numerator (n_i) and denominator (d_i) of the controller for the aperture of the expansion valve besides the constants of the PI controller for the compressor speed. For the second scenario, the evolutionary individual is built by the constants of the PID_i controllers for both variables (see **Table 3**). Behavioral paths arise from direct experimentation on the benchmark model, subsequently the error of the control variables in relation to each reference change is calculated.

Table 3. Individual structure for the first (default) and second (new) scenarios.

1st Scenario	2nd Scenario
(n_1, n_2, d_1) $\in \mathbb{R}$	(P_1, I_1, D_1) & (P_2, I_2, D_2) $\in \mathbb{R}$
(n_3, d_2), (P, I) $\in \mathbb{R}^+$	

Errors e_{Te1} and e_{Te2} correspond to the two reference changes for the evaporator outlet temperature. See **Eqs. (6)-(7)**. e_{Tsh1}, e_{Tsh2}, e_{Tsh3}, e_{Tsh4} correspond to the four reference changes for the super heat temperature, see **Eqs. (8)-(11)**. The final performance index (ITAE) is **Eq. (12)**.

$$e_{Te1} = \int t_{e1} * |r_{e1} - T_{e1}| \quad (6)$$

$$e_{Te2} = \int t_{e2} * |r_{e2} - T_{e2}| \quad (7)$$

$$e_{Tsh1} = \int t_{sh1} * |r_{sh1} - T_{sh1}| \quad (8)$$

$$e_{Tsh2} = \int t_{sh2} * |r_{sh2} - T_{sh2}| \quad (9)$$

$$e_{Tsh3} = \int t_{sh3} * |r_{sh3} - T_{sh3}| \quad (10)$$

$$e_{Tsh4} = \int t_{sh4} * |r_{sh4} - T_{sh4}| \quad (11)$$

$$J_{ITAE} = \sqrt{e_{Te1}{}^2 + e_{Te2}{}^2 + e_{Tsh1}{}^2 + e_{Tsh2}{}^2 e_{Tsh3}{}^2 + e_{Tsh4}{}^2} \quad (12)$$

The challenge involves minimizing the ITAE cost function while determining the settings for both controllers. This objective requires finding optimal parameter magnitudes for each controller to quickly reach the desired reference values, r(t), for both the cooling demand and the degree of superheating, with minimal oscillations. The objective function in MAGO for each scenario is in **Eqs. (13)-(14)**.

$$J\,(n_1, n_2, n_3, d_1, d_2, P, I) = \min\{J_{ITAE}\} \quad (13)$$

$$J\,(P_1, I_1, D_1, P_2, I_2, D_2) = \min\{J_{ITAE}\} \quad (14)$$

Both controllers operate simultaneously on the plant, generating deviations from the reference values of the study variables. These deviations are calculated individually at each time instant and combined to form the total system error. By incorporating all reference errors into a single cost function, the inherent coupling of the problem variables is accounted for. MAGO minimizes the ITAE while considering the interdependence among variables when estimating controller parameters. A new set of controllers is iteratively adjusted to reduce deviations from the desired behavior until a stopping criterion is met. This iterative process remains consistent regardless of the controller or plant model structure or domain. The problem statement for the two new continuous controllers for the benchmark is as follows: $\boldsymbol{\Sigma}_{vcrs} = (\boldsymbol{T}, \boldsymbol{W}_{vcrs}, \boldsymbol{\mathcal{B}}_{bmark})$, where $\boldsymbol{T} \in \mathbb{R}$, $\boldsymbol{W}_{vcrs} \in \mathbb{R}^{\boldsymbol{4}}$, $\boldsymbol{\mathcal{B}}_{bmark} = (AV, N, T_{e,sec,out}, T_{sh})$ and $\boldsymbol{\mathcal{B}}_{bmark} \subset \mathbb{R}^{\boldsymbol{qT}}$, with $\boldsymbol{\mathcal{B}}_{bmark}$ subject to the constraints from the IFAC PID18 benchmark. $w(i) = \begin{bmatrix} u(i) \\ y(i) \end{bmatrix}$ with $u(i)=(AV,\ N)$, $y(i)=(T_{e,sec,out}, T_{sh})$ *all* $\in \mathbb{R}$. The controlled problem is then $\sum_{kvcrs} = (\boldsymbol{\mathcal{B}}_{kAV} \text{ X } \boldsymbol{\mathcal{B}}_{kN}) \Lambda \boldsymbol{\mathcal{B}}_{kbmark}$.

Each $\boldsymbol{\mathcal{B}}_{ki} = (P_i,\ I_i,\ K_i) \in \mathbb{R}$, and $e_i(t) = (w_i - \text{wr})$.

$$\underset{\substack{w \in W \\ (K_{P(i)}, K_{I(i)}, K_{D(i)}) \in \mathbb{R},\ i=AV,N \\ Wr \in \boldsymbol{\mathcal{B}}^{Ref}}}{\text{minimize}} \quad C_{control}\ (w - w_r)$$

Subject to $w = \begin{bmatrix} u_{(t)} \\ y_{(t)} \end{bmatrix} = \begin{bmatrix} AV_{(t)} & N_{(t)} \\ Te, sec, out_{(t)} & Tsh_{(t)} \end{bmatrix} \in \boldsymbol{\mathcal{B}}_{bmark}$

$u_i(t) = \text{F}(e_i(t)) = \text{Kp}_i(t).e_i(t) + \text{Ki}_i(t). \int e_i(t) + Kp_i(t).\frac{d}{dt} e_i(t)$

$(Te, sec, out_{Ref} - Te, sec, out_{(t)}) \rightarrow 0$, $(Tsh_{Ref} - Tsh_{(t)}) \rightarrow 0$

4. Analysis of Results

The results obtained through the behavior-based control by evolutionary learning of trajectories proposed in this work are highlighted below. MAGO input data are in **Table 4**. The simulation process involved an exhaustive search to find a specific solution for the VCRS controllers. Using an Intel Xeon CPU @ 2.30GHz with 7.20GB of RAM and 64-bit architecture, the average execution time was 9 hours. This long execution time is due to the fact that no preprocessing of the initial population was performed, reflecting the real complexity of the problem and the intensive exploration of the search space to find an optimal solution. The process was carried out autonomously and monolithically, without relying on parallelization or external resources for execution.

Table 4. MAGO input data for the first and second scenarios.

Data	1st Scenario	2nd Scenario
Individuals	50	50
Generations	25	25
Upper bound	[5 1 1 5 1 1 1]	[20 10 1 20 10 1]
Lower bound	[-5 -1 0 -5 0 0 0]	[-20 -10 -1 -20 -10 -1]

Parameters derived from the behavior-based approach for both the discrete TF controller and the continuous coupled PID controllers are displayed in **Table 5**. For the first scenario (benchmark default), **Figures 5 to 9** show the system behavior paths and their corresponding efficiency indices under both the benchmark strategy and the behavior-based control through evolutionary learning of trajectories. For the second scenario (new coupled continuous PID controllers), the paths and efficiency indices are illustrated in **Figures 10 to 14**. In these figures, the dashed line represents the reference, blue line depicts the default controller, and red line represents the behavior-based evolutionary controllers.

Table 5. Parameters found through the behavior-based approach for the first and second scenarios.

Controller	1st Scenario Discrete Transfer Function	2nd Scenario Continuous coupled PID
Te,sec,out – Av	$\frac{-1.1036 - 0.0626z^{-1} + 0.9977z^{-2}}{1 - 1.9853z^{-1} + 0.9853z^{-2}}$	$P_1 = 13.1978$ $I_1 = -3.000$ $D_1 = 0.0481$
Tsh – N	P=0.42 I=0.9967	$P_2 = 4.9996$ $I_2 = 4.7378$ $D_2 = 0.0209$

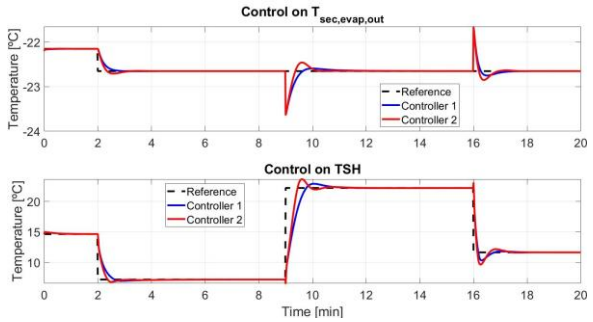

Fig. 5. Controlled variables for default discrete transfer function controller (blue line benchmark strategy | red line behavior-based control).

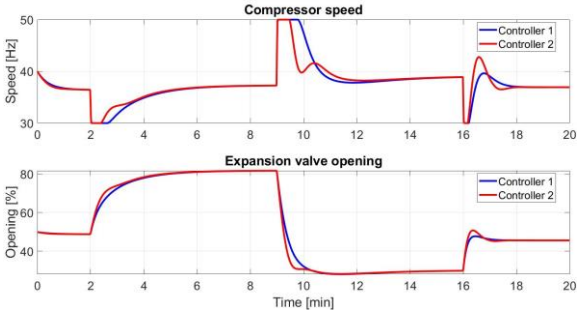

Fig. 6. Manipulated variables for default discrete transfer function controller (blue line benchmark strategy | red line behavior-based control).

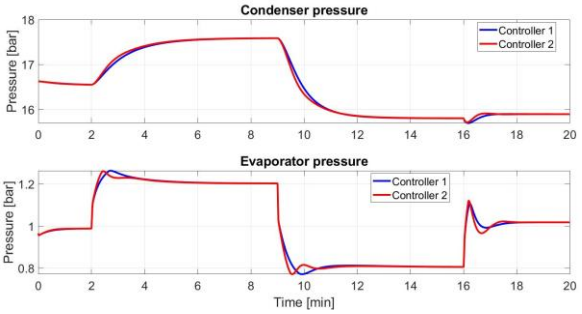

Fig. 7. Evaporation and condensation pressures for default discrete transfer function controller (blue line benchmark strategy | red line behavior-based control).

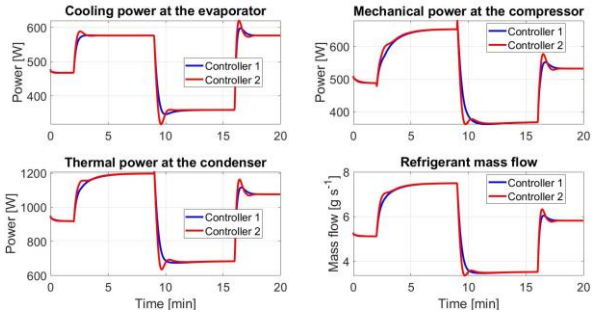

Fig. 8. Thermal power at each component and refrigerant mass flows for default discrete transfer function controller (blue line benchmark strategy | red line behavior-based control).

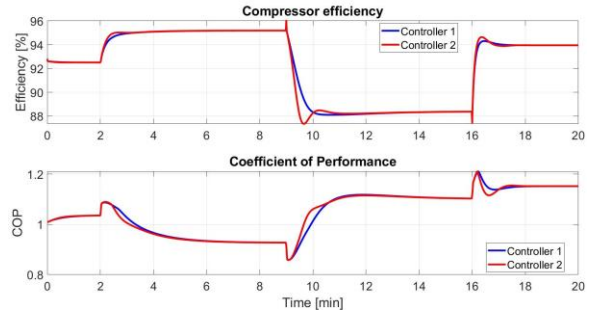

Fig. 9. Compressor efficiency and coefficient of performance for default discrete transfer function controller (blue line benchmark strategy | red line behavior base control).

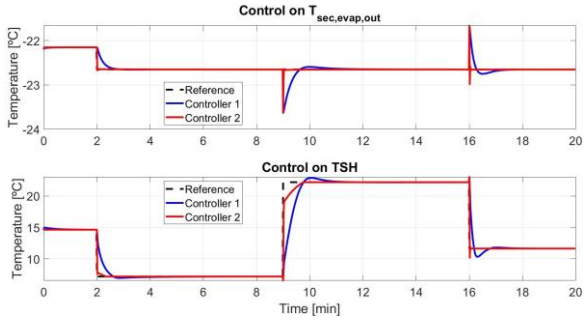

Fig. 10. Controlled variables for new continuous PID controller (blue line benchmark strategy | red line behavior-based control).

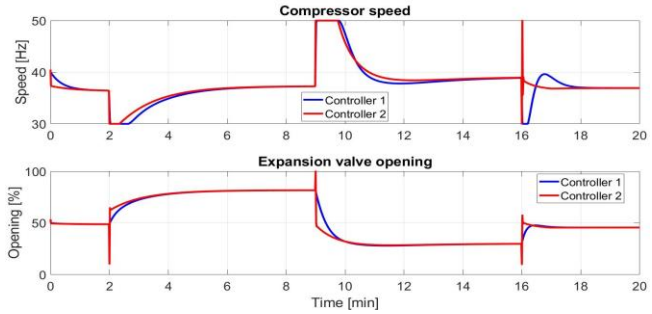

Fig. 11. Manipulated variables for new continuous PID controller (blue line benchmark strategy | red line behavior-based control).

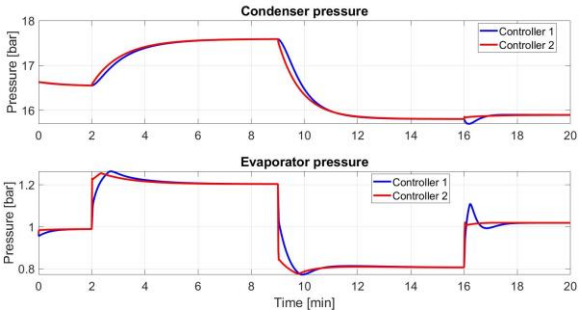

Fig. 12. Evaporation and condensation pressures for new continuous PID controller (blue line benchmark strategy | red line behavior-based control).

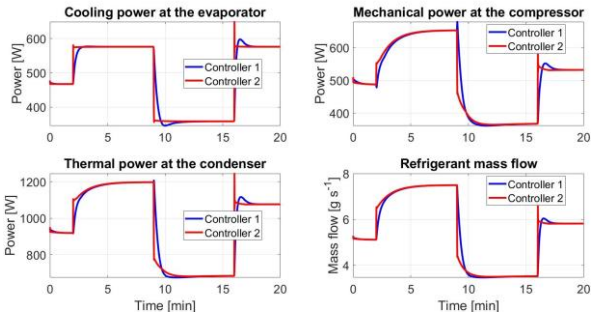

Fig. 13. Thermal power at each component and refrigerant mass flows for new continuous PID controller (blue line benchmark strategy | red line behavior-based control).

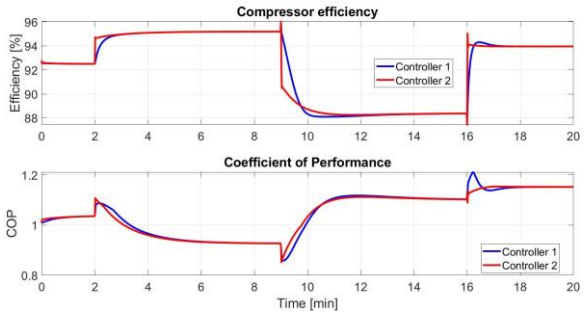

Fig. 14. Compressor efficiency and coefficient of performance for new continuous PID controller (blue line benchmark strategy | red line behavior-based control).

Relative and combined indices associated to the scenario's comparison, default benchmark controllers vs. both behavior-based approach, are in **Table 6**. A detailed description of those indices, comparing strategies, including MAGO, presented to the benchmark challenge, is in (Viola et al., 2018).

The benchmark creators defined the indices in Table 6, and their weights are unknown for the benchmark users. Those indices assess the ratio of the integral absolute error (RIAE), the ratio of integral time absolute error (RIT AE), and the ratio of integral absolute variation of the control signal (RIAVUi) between the decentralized default controllers and the proposed controllers. To measure the global performance of the system the index J(c2, c1) was considered.

Table 6. Relative and combined indices to the comparison between default benchmark controllers vs. behavior-based approach.

C1: benchmark default 1 (controllers of reference)
C2: behavior-based proposal (controllers to evaluate)

Index	TF	PID
RIAE1(C2,C1) Te,sec,out	0.9371	0.1223
RIAE2(C2,C1) TSH	0.8394	0.2273
RITAE1(C2,C1,tc1,ts1) Te,sec,out	1.1835	0.3789
RITAE2(C2,C1,tc2,ts2) T_{SH}	0.7353	0.0274
RITAE2(C2,C1,tc3,ts3) T_{SH}	0.6540	0.1439
RITAE2(C2,C1,tc4,ts4) T_{SH}	1.3447	0.0126
RIAVU1(C2,C1) Av	1.0601	2.6656
RIAVU2(C2,C1) N	1.1556	1.4477
J(C2,C1)	0.9894	0.3204

For the first strategy (discrete transfer function controllers) it is observed through indices 1 and 2 a higher performance of the controller in reaching the reference for the output variables of the VCRS. Similarly, there is a substantial improvement in the handling of the reference changes for *Tsh*, highlighting its effectiveness for the first two. Finally, the global index numerical value shows a slight improvement in relation to the benchmark reference controller. For the second strategy (continuous coupled PID controllers), in general terms, it is possible to increase the precision of the controller for both reaching the reference of the output variables as well as showing great adaptability and precision in the presence of reference changes. The general indicator J establishes a significant increase in the performance of the controller for this exercise. Additionally, by reducing energy consumption in a system under identical operating conditions, as per Lyapunov's energy principle, implies increased stability, indicating higher efficiency and resilience to external disturbances. However, despite the good results, these controllers could be improved to achieve a smoother manipulation of actuators.

Table 7. ITAE and relative index proposal

Index	**TF** (default)	**TF** (behaviour-based)	**PID** (behaviour-based)
J(ITAE)	1.7620e+05	1.4852e+05	4.0724e+04
Relative Index	1.000	0.843	0.231

An easy-of-use index, **Eq. (14)**, to assess the performance of each control scheme throughout the whole simulation period is shown in **Table 7**. The behavior-based control clearly outperforms the classical method.

5. Conclusions

The behavior-based approach through evolutionary learning of trajectories offers a significant advantage due to its direct connection with the actual system, regardless of its representation or controller structure, thus emulating real physical conditions for experimental purposes and accommodating any control scheme. By nature, this approach ensures only feasible solutions, guiding the controller towards desired conditions. It reduces the analyst's effort in handling complex coupled MIMO systems by transferring it to the machine learning process. Control by evolutionary learning of behaviors applies the same methodology whether a model or only data is available. Compared to the benchmark control strategy the coupled continuous controllers identified in this study significantly outperformed the same performance criteria. Future developments should address high variations in manipulated variables to mitigate potential component deterioration and optimize the performance of continuous PID controllers by issues like derivative and integral terms to ensure compatibility with implementable industrial systems.

References

Balarezo-Gallardo, S.-F., & Hernández-Riveros, J. A. (2017). Evolutionary Parameter Estimation of Coupled Non-linear Oscillators. In A. Solano & H. Ordoñez (Eds.), *Advances in Computing* (pp. 457–471). Springer I. P.

Bejarano, G., Alfaya, J. A., Rodríguez, D., Ortega, M. G., & Morilla, F. (2018). *BENCHMARK PID 2018 Benchmark for PID control of refrigeration systems based on vapour compression* (pp. 1–20).

Hernández-Riveros, J. A. & Cano, D. V., 2012, *Advances in Artificial Intelligence, IBERAMIA 2012 - 13th Ibero-American Conference on AI, Proceedings.* Springer Verlag, p. 271-280 10 p. (LNAI, vol. 7637).

Hernández-Riveros, J.-A., Urrea-Quintero, J.-H., & Carmona-Cadavid, C.-V. (2016). Evolutionary Tuning of Optimal PID Controllers for Second Order Systems Plus Time Delay. In J. J. Merelo, A. Rosa, J. M. Cadenas, A. Dourado, K. Madani, & J. Filipe (Eds.), *Computational Intelligence* (pp. 3–20). Springer I. P.

Li, B., Jain, N., Mohs, B., Munns, S., Patnaik, V., Berge, J., & Alleyne, A. G. (2012). Dynamic modeling of refrigerated transport systems with cooling-mode/heating-mode switch operations. *HVAC and R Research*, *18*, 974–996. https://doi.org/10.1080/10789669.2012.670685

Schurt, L. C., Hermes, C. J. L., & Neto, A. T. (2009). A model-driven multivariable controller for vapor compression refrigeration systems. *International Journal of Refrigeration*, *32*(7), 1672–1682. https://doi.org/10.1016/j.ijrefrig.2009.04.004

Soto, G. J. A., López, J. M. G., & Hernández-Riveros, J. A. (2018). Coupled evolutionary tuning of PID Controllers for the Benchmark on Vapor Compression Refrigeration. *IFAC-PapersOnLine*, *51*(4), 509–514. https://doi.org/10.1016/j.ifacol.2018.06.146

Viola, J., Radici, A., & Chen, Y. (2018). Comparison of control strategies for the temperature control of a refrigeration system based on vapor compression. *ArXiv:1810.06074 [Cs]*. http://arxiv.org/abs/1810.06074

Willems, J. C. (2007). The Behavioral Approach to Open and Interconnected Systems. *IEEE Control Systems*, *27*(6), 46–99. https://doi.org/10.1109/MCS.2007.906923

Zardini, G. (2017). Control Systems II. *Systems Engineering*, *January,* 1–78.

Zeng, G., Chen, J., Chen, M., Dai, Y., Li, L., Lu, K., & Zheng, C. (2015). Multivariable PID controllers using real-coded population-based extremal optimization. *Neurocomputing*, *151*, 1343–1353. doi.org/https://doi.org/10.1016/j.neucom.2014.10.060